EFFECT OF Al_2O_3 PARTICULATES ON THE PROPERTIES OF THE SINTERED Al-Zn-Mg-Cu-Ni-Co ALLOY AFTER T6 AND RRA TREATMENTS

H. T. NAEEM[a,b*], K. S. MOHAMMED[a]
[a]*School of Materials Engineering, University Malaysia Perils, Jejawi, Perlis, Malaysia*
[b]*Chemical Engineering, College of Engineering, Al-Muthana University, Muthana, Iraq*

In this study, the effects of Alumina particles on the microstructure and the hardness of experimental an Al-Zn-Mg-Cu-Fe-Cr-Ni-Co matrix alloy was produced using powder metallurgy. Aluminum matrix composite reinforced with Al_2O_3 particles of volume fraction 5% with average size about 4μm was investigated. The prepared composite powders were consolidated by cold pressing and then the sintered. The sintered composite samples have been subjected to a homogenization treated then aged at (T6 temper) and retrogressed, and then re-aged (RRA). The results indicated that the T6 heat treatment increases the hardness of an Al-composite compared to be as sintered. With applying the retrogression and reging process, aluminum matrix composite has the highest hardness. This improvement of microhardness attributed to the precipitation hardening from having of MgZn, Mg_2Zn_{11} phases, additionally the dispersion strengthening of Al_2O_{3P}, Ni and/or Co-dispersoid intermetallic compound in the matrix. Microstructure characterization of an Aluminum matrix composite was carried out using optical microscopy (OM), scanning electron microscopy (SEM), energy dispersive spectroscopy (EDS) and X-ray diffraction (XRD.

(Received February 4, 2015; Accepted April 29, 2015)

Keywords: Al-Zn-Mg-Cu-Ni matrix alloy; Alumina particulates; RRA treatments.

1. Introduction

Al-Al2O3 composites are an important member of the metal matrix composites (AMCs) and are widely being used in the in aviation, transportation, and military industries. These materials have received large demand due to their improved mechanical, tribological and high temperature properties [1-3]. Previous studies indicated that the use different ceramic particles as reinforcing materials within Aluminum PM Alloys such as Al_2O_3 [4], SiC_p [5], MgO [6]. Between these aluminum alloys, the 7xxx series refers to a high response to compaction and sintering process besides development of their properties with using ceramic in particles form [7, 8]. In the past time, there are some investigations on the effect of heat treatment on the mechanical properties of AMCs that are responsive to heat treatment [9, 10, and 11]. Thus based to some of the outcomes; it is possible to improve the mechanical properties of such a AMCs with the aging. In the present study, Al-Zn-Mg-Cu-Fe-Cr matrix alloy produced via conventional powder metallurgy from elemental powders equivalent to the 7xxx Al-alloy, (i.e. AMC heat treatable), the aging, retrogression and reaging treatment were carried on this AMC. The aim of this work, effects of alumina on the properties of Al-Zn-Mg-Cu-Fe-Cr matrix alloy containing additives of nickel and cobalt; after undergoing the sintering condition then series of heat treatment.

*Corresponding author: haider_neem@yahoo.com

2. Experimental Work

2.1 Raw Materials

The PM alloy in this research namely (alloy E) has a nominal compositions of Al-5.5Zn-2.5Mg-1.5Cu-0.4Fe-0.2Cr-1Ni-1Co-5Al_2O_3 (wt.%) were compacted from premixed, characteristics of the elemental powders is given in Table 1; Particle size distribution was measured by Malvern Mastersizer 2000 powder size analyzer.

Table 1: Starting powder characteristics

Powder	Description	Powder sizes (µm)	Purity	Source
Al	Flake	D50 of 51 µm	98%	Merck KGaA
Al_2O_3	Rounded	D50 of 4 µm	99.5%	Merck KGaA
Zn	Rounded	D50 of 18 µm	96 %	Merck KGaA
Mg	Rounded	D50 of 115 µm	98 %	Merck KGaA
Cu	Irregular	D50 of 39 µm	99.5%	Merck KGaA
Fe	Rounded	D50 of 200 µm	99.5%	Merck KGaA
Cr	Irregular	D50 of 160 µm	99.5%	Merck KGaA
Ni	Rounded	D50 of 11 µm	99.5%	Merck KGaA
Co	Fine particle	D50 of 750 µm	99.5%	Merck KGaA

2.2 Procedures of Techniques

The PM processing is mixing route followed in this study which included powder blending, uni-axial die compaction and controlled atmosphere sintering. All powders were initially blended in a Turbula mixer for twenty minutes. The mixed of mixture powders was cold press in a cylindrical steel mould has a die Ø 16-mm under the pressure was about 360 MPa using a floating uniaxial die a hand-operated hydraulic cold press to make the green compact. The sample has weighed approximately, 3.5 grams. Thereafter the green compacts were sintered in LT the tubular furnace under the pure argon gas atmosphere. The sintering process was started from 25°C to 650°C for 120 minutes (soaking time). The heating rate during sintering was about 8°C/min. The sintering densities and total porosity of the compact samples were determined using the Archimedes principle according to the ASTM B 312-09 [12]. After the sintering process accomplished, the compacts were homogenization treated followed by quenching in water immediately. To the further optimization, the samples were performed the aging at T6 temper and was then the retrogression and re-aging process followed by quenching in cold water after each step of the heat treatments respectively, according to the procedures as shown in Figure 1.

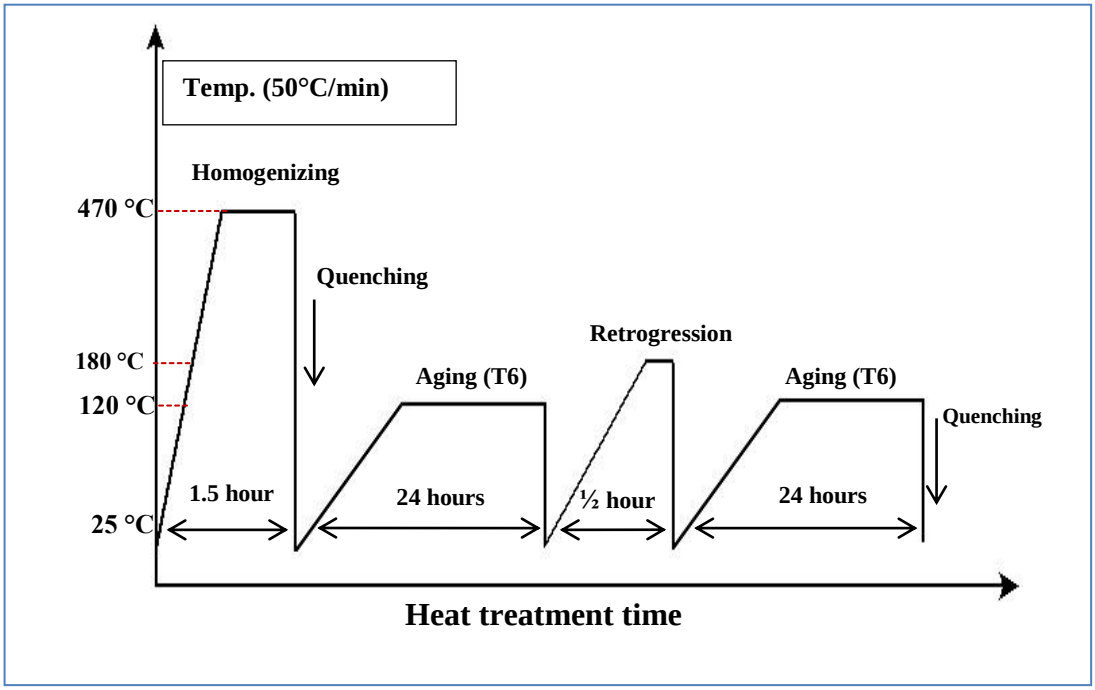

Fig. 1. Schematic of heat treatment cycle of the alloy E.

Vickers Hardness of the sintered and the heat treated alloy E samples was measured using "Mitutoyo DX256 series", where indentation force was set to be 20N, and 10 second dwelled time. To ensure cleanliness the surfaces of the compacts were polished prior to HV measurement. Each reading was an average of at least ten separate measurements taken randomly. Characterizations of microstructure of the alloy E samples were analyzed by the optical microscopy (OM) using (Olympus PMG3 optical microscope), scanning electron microscopy ((SEM) JEOL JSM-6460LA analytical scanning electron microscope) coupled energy dispersive X-ray spectroscope (EDS) and X-ray diffraction analysis was ((XRD) SHIMADZU, and X-Ray Diffractometer) used under the following conditions; scan range: 20°-80°, step size: 0.03, scan rate: 5°/min.

3. Results and discussion

Fig. 2 (a), (b) and (c) shows optical microstructures of the mixed alloy E composites underwent the sintering process, the aging at T6 temper and the RRA treatment, respectively. It can be observed that clusters of alumina particles were distributed sufficiently uniformly within matrix of the mixed alloyE composite in addition to the presence a little of pores in matrix. The average sintered density of the alloy E was determined to be 2.581 g/cm^3 representing 83 % of the theoretical density 3.110 g/cm^3, respectively. Meanwhile, the total residual porosity within the sintered alloy E were calculated to be about 17%. The presence of porosity of the alloy E composites attributed to reason agglomeration of alumina particulates which had formed the pores irrespective to the sintering conditions.

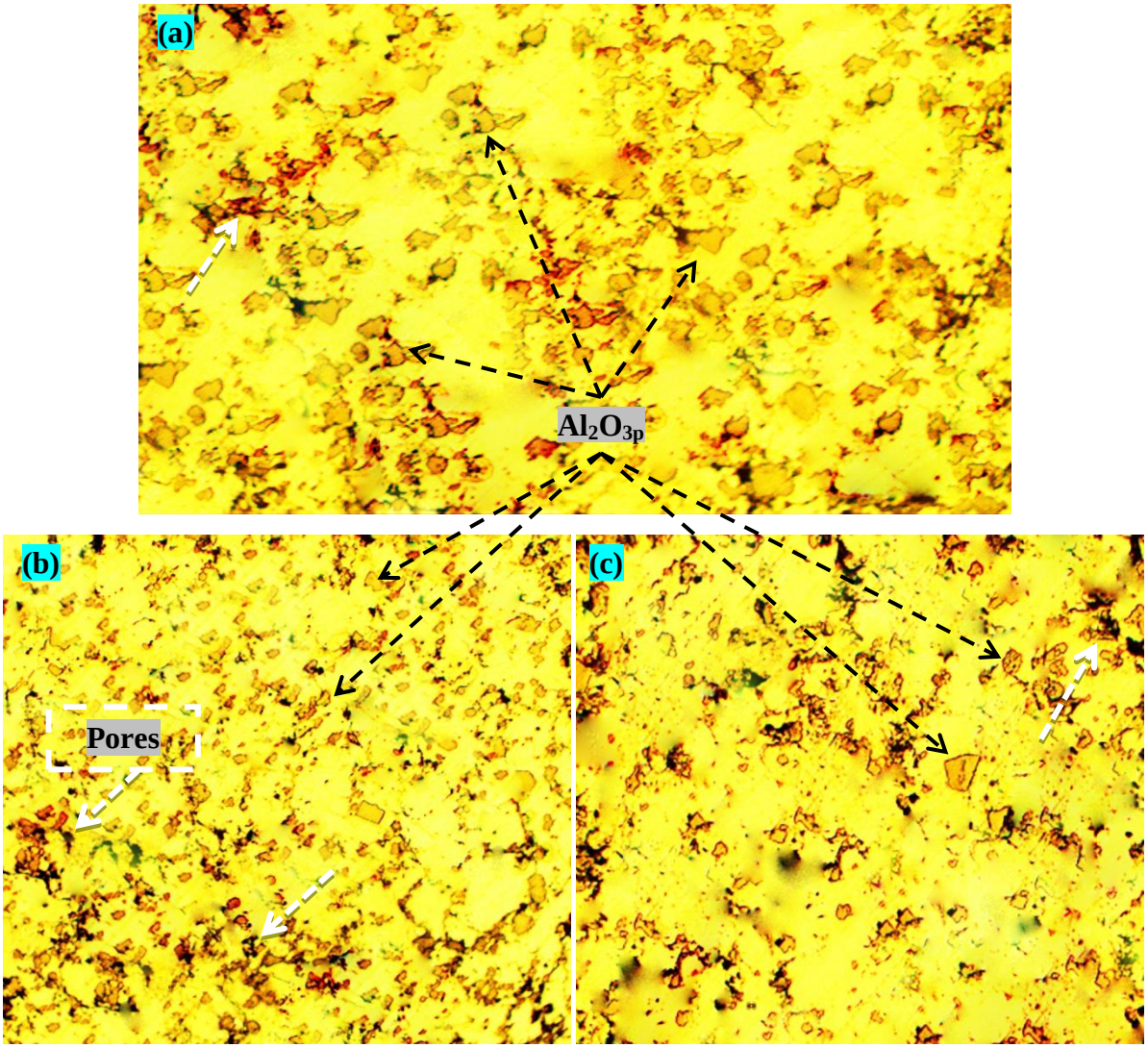

Fig. 2: Optical microstructure of the mixed alloy E; after (a) the sintering, (b) T6 and (c) RRA

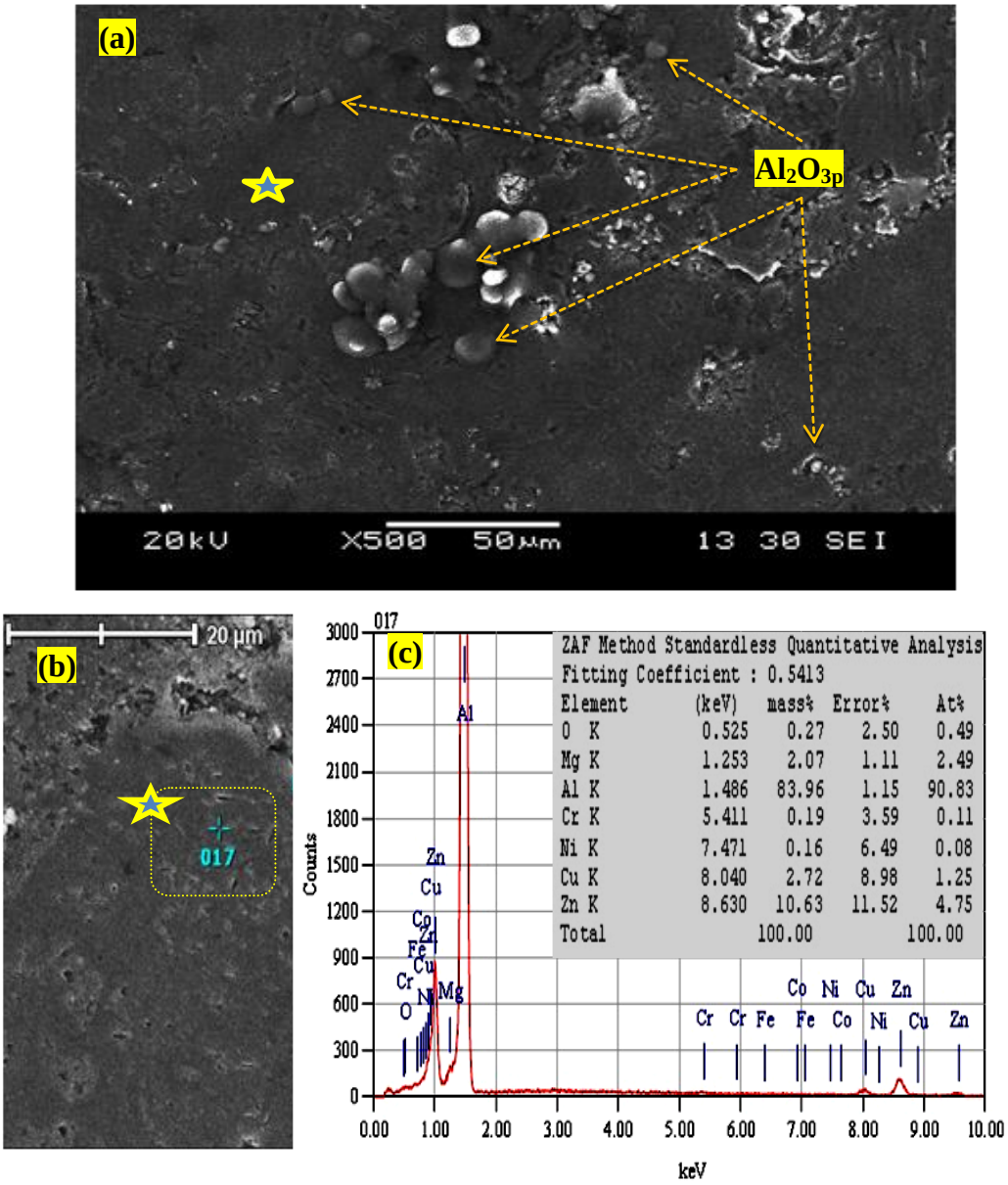

Fig. 3: (a-b) SEM micrograph and (c) EDS scan analysis of the mixed alloy E after the sintering process.

To evaluate the microstructure of the mixed alloy E composite, the SEM presents in Figure 3(a) indicates that the distribution of Al_2O_3 particles within the matrix is reasonably uniform with some of agglomeration of particles. Also, it is obviously that alumina particles in matrix which reveals a good interfacial and bonding between the reinforcement Al_2O_{3p} and the matrix of alloy E that attributed to the existence alloying element of Mg in composites as have conducted by [13].

Furthermore, Cheng et al and Rahimian et al [14-15] observed that a good interfacial bonding is achieved between the Al_2O_3 particulates and aluminium alloy matrix due to the small Al_2O_{3p} (4 µm) and an advanced sintering processat an elevated temperatures. Therefore, the role interface is the most important affecting in mechanical properties of Al-composites. Figure 3(b) shows the enlarged supplementary SEM image of the alloy E matrix. The EDS scan analyses of the labeled regions as shown in Figures 3(c) indicate that the chemical compositions coexist of alloying elements with content of nickel.

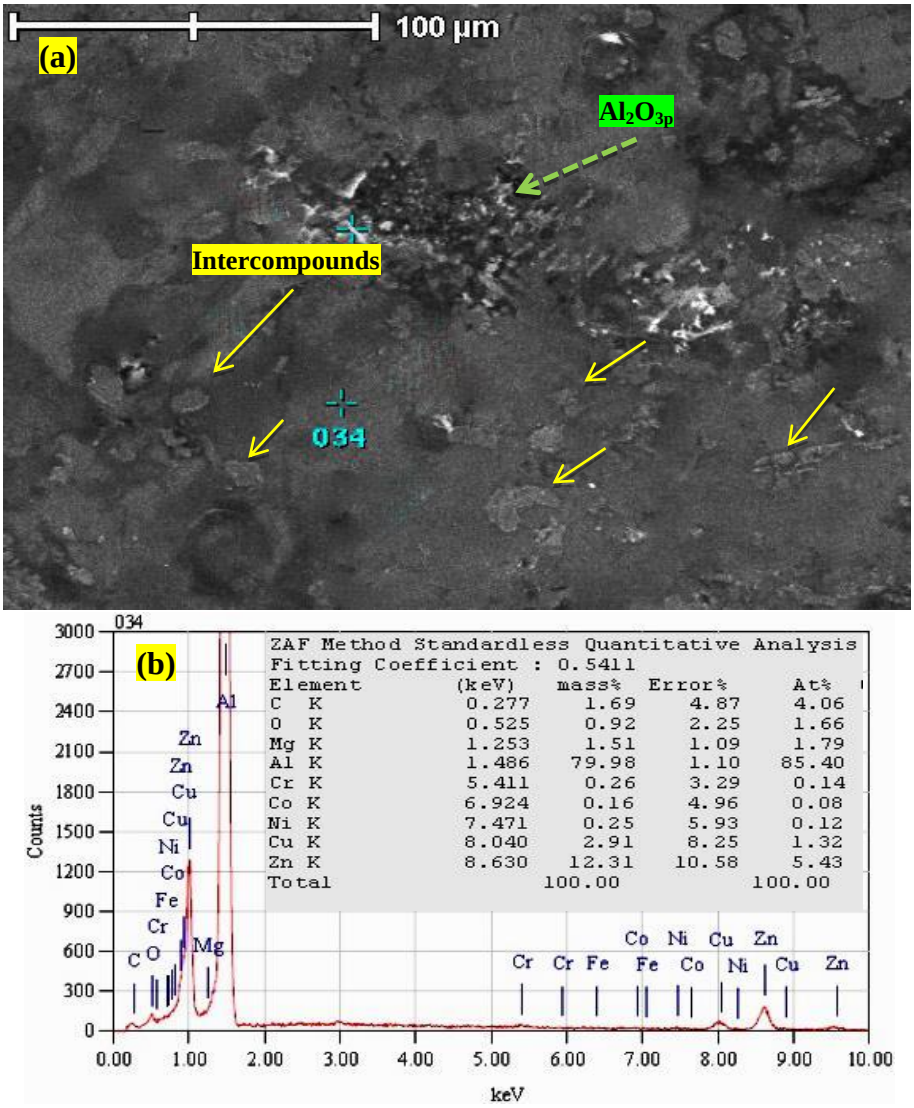

Fig. 4: (a) SEM micrograph and (b) the EDS scan analysis of the mixed alloy E underwent the T6 temper.

SEM micrograph of the mixed alloy E composite after the aging at T6 is given in Figure 4 (a) indicates the embedded of alumina particle in matrix as well as good distributed in addition to the presence of intermetallic compounds of Ni, Co and precipitates of alloying elements within matrix. The EDS microanalysis detects the composition of the numbered spot in matrix as given in Figure 4 (b).

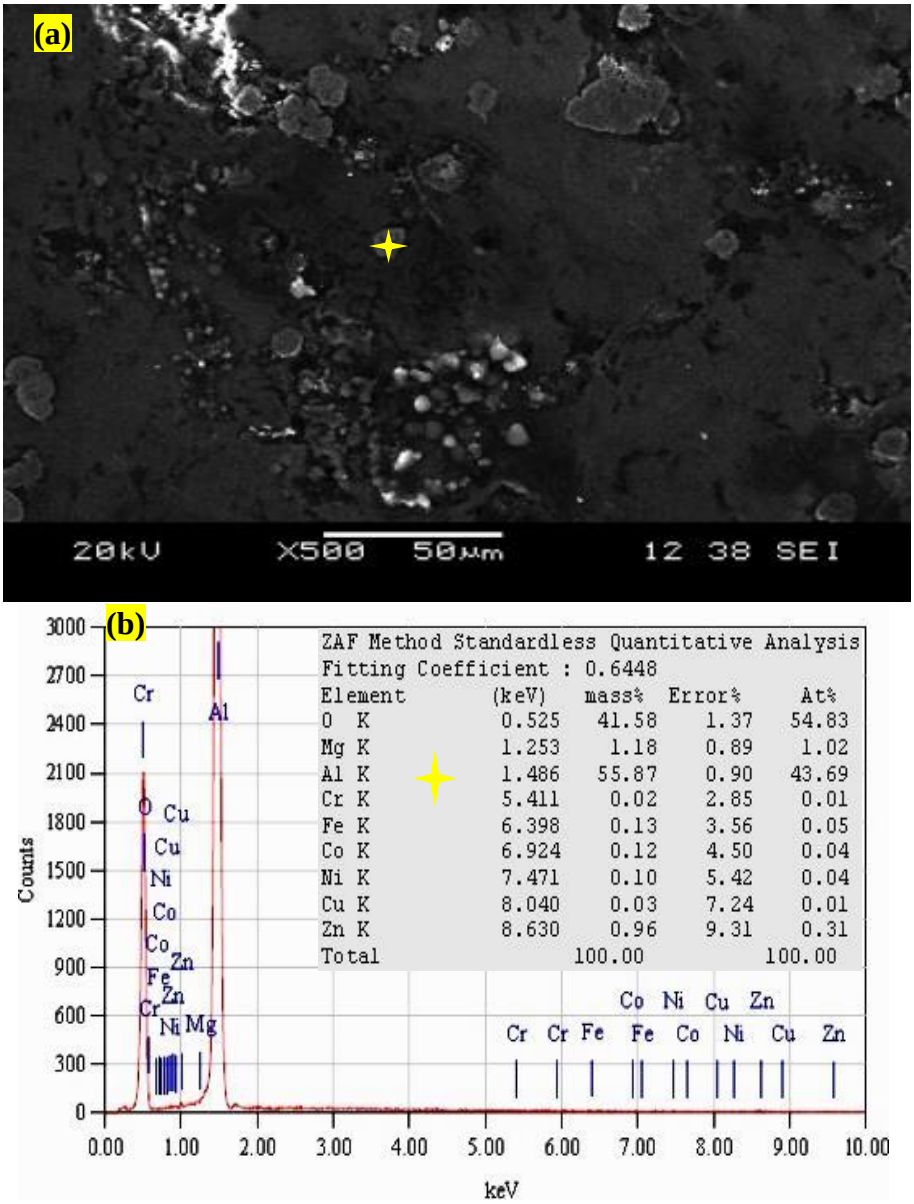

Fig. 5: (a) SEM micrograph and (b) EDS of the mixed alloy E underwent the RRA.

Fig. 5 (a) show the SEM micrograph of the PM alloy E composite after the RRA. It can be observed the bright spots as alumina particle in matrix and also some agglomerated of alumina. Figure 5 (b) presents the EDS microanalysis of the labeled region which is intermetallic compounds dispersed within matrix.

Fig. 6 show the XRD patterns of the mixed alloy E composite after the sintering; the T6 temper, and the RRA process. Figure 6(c) refers to the sintered alloy E composite sample which fundamentally consisted of the AlZn and MgZn in addition to the appearing phases of Al_5Co_2, Al_2O_3 and intermetallic compound (i.e. Al_4Ni_3). The generally the precipitation hardening sequences for the 7XXX series aluminium alloys are as follows: [16-17]: supersaturated solid solution → coherent stable Guinier–Preston (GP) zones→ semi-coherent intermediate η′-phase→ Metastable stable η-phase. The primary precipitations in the matrix are the GP zones and η′-phase undergone the aging at 120 °C for 24 hours. Figure 6(b) the XRD patterns of the mixed alloy E composite sample after the T6. It is noticed that the major peaks of Mg_2Zn_{11} and AlZn were achieved while there having of phases of Al_2O_3, $Al_{70}Co_{20}Ni_{10}$, Al_5Co_2, and Al_4Ni_3. Figure 6(a) exhibit the XRD analysis of the alloy E sample after the RRA process. It can be seen that the main peaks are the Mg_2Zn_{11} and AlZn as well as the secondary peak of the $Al_{70}Co_{20}Ni_{10}$. Also, the

plenty of η′-Mg_2Zn_{11} phases compared with the T6 due to the RRA mechanisms as mentioned former. Also, it can be noted that the new Al_3Ni_2 phase created besides phases have already found (i.e. Al_4Ni_3, Al_5Co_2 and Al_2O_3). The precipitation procedure through the matrix of an Al-Zn-Mg-Cu alloy after carrying the RRA process is more detailed by [8, 17-18].

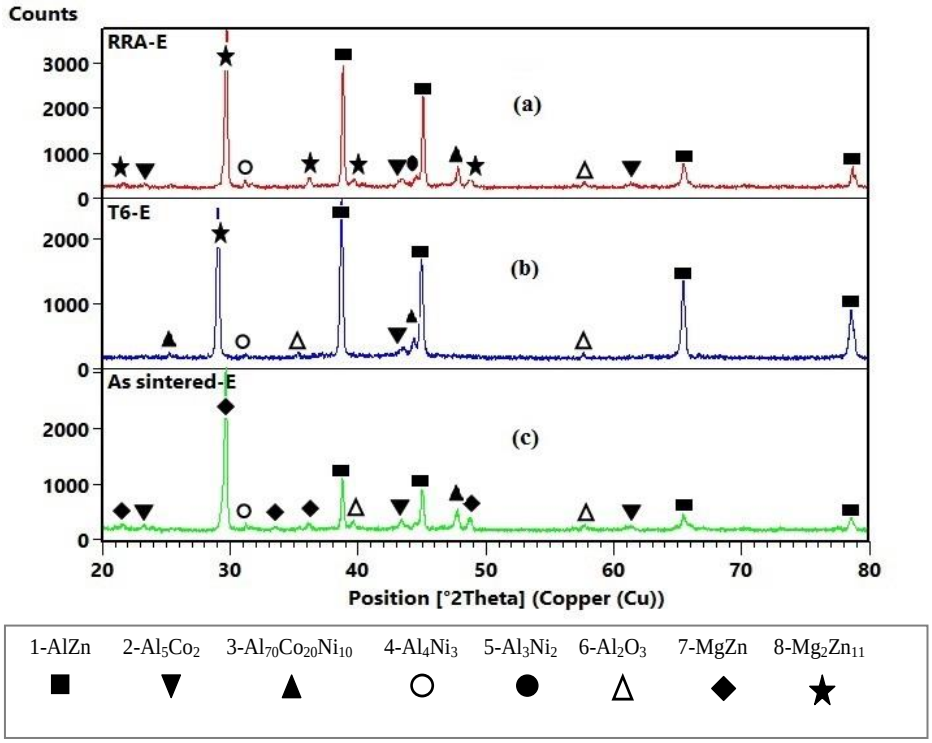

Fig. 6: The XRD plots of the mixed alloy E composite; after the sintering, T6 and the RRA process.

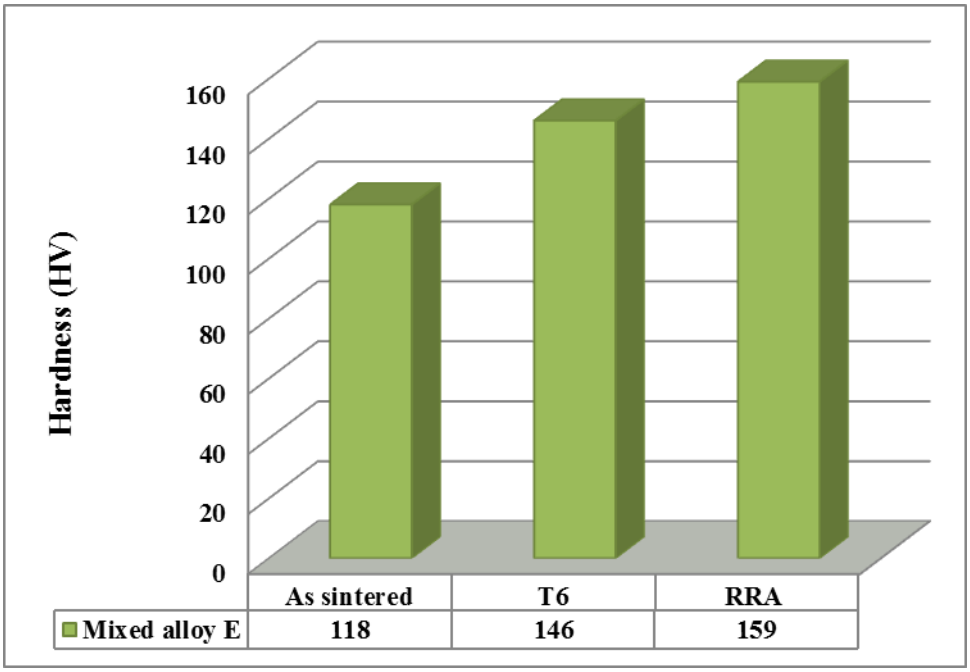

Fig. 7: Vickers hardness values of the alloy E composite sample after different heat treatment conditions.

As it is expected, the hardness measurements verify that the hardness alloy E composite sample's increases from average value of 118 HV (as sintered) to 146 and 159 HV after carrying T6 temper and RRA process, respectively. It can be explained with respect to the distribution of the hard second phase Al_2O_3 particles within the matrix as well as having intermetallic compounds (i.e. $Al_{70}Co_{20}Ni_{10}$, Al_5Co_2, Al_3Ni_2 and Al_4Ni_3). Thus, the results show that the hardness of the composite that subjected to the aging at T6 temper, and the RRA is more than the composite as sintered. The findings of this study contrary with the outcomes by Dasgupta [8] showed that an Al-Zn-Mg-Cu matrix composite under the RRA treatment has not given higher hardness.

Improvement of the hardness can be attributed to three phenomena:

1. The precipitation hardening detailed as mentioned a former above.
2. The dispersion strengthening is described that as the addition of alumina particles to aluminum P/M alloy matrix with good distribution and interfacial bonding as well as the existence of Ni plus cobalt dispersoids particles within the matrix.

The dispersion is attributed to the effects of average alumina particle size of 4µm. Delicate description on Eq. (1) Refer that the distance apart from the reinforcement is reduced while using finer powders as mentioned by [19].

$$\lambda = \frac{4(1-f)r}{3f} \tag{1}$$

Where λ is the distance apart from the reinforcements, f is the fractional volume of the reinforcement; r is the radius of the particles (assuming them spherical). When alumina particles act as a barrier during deformation, according to Eq. (2), more energy is required in the movement of dislocations when they encounter a finer hard phase [15, 20-21].

$$\tau_0 = \frac{G\,b}{\lambda} \tag{2}$$

Where $\tau_0$is the stress required for a dislocation to pass reinforcement, *G* is the shear modulus of the material and *b* is the Berger's vector of the dislocation.

3. Strengthening occurred is due to the coefficient of thermal expansion (CTE) mismatch between the matrix and the reinforcement of alumina, which resulted in a high dislocation density in the matrix.

4. Conclusions

In this research, effectiveness of alumina dispersoids within Al-Zn-Mg-Cu-Ni-Co matrix alloy under the heat treatments was investigated. The findings can be summarized as followings:

1. The relative density of Al-alloy/Al_2O_3 composite was the high due the containing fine particle sizes.
2. Regarding of the microstructures and the XRD analysis of an Al-Zn-Mg-Cu- Ni-Co alloy/Al2O3 composite samples that appearing a variety of precipitates including the GP zones and η′-Mg_2Zn_{11} phases with existence the intermetallic dispersion as $Al_{70}Co_{20}Ni_{10}$, Al_5Co_2, Al_3Ni_2 and Al_4Ni_3 as well as having Al_2O_3 hard second phase.
3. The highest hardness was 159 HV in Aluminum-alloy specimens containing average alumina particle size of 4µm heated at the retrogression and reaging (120 °C for 24 h +180°C for 30 min. + 120 °C for 24 h).

Acknowledgements

This work is supported under the University Malaysia Perlis (UniMAP).

References

[1] M. Rezayat, A. Akbarzadeh, Materials and Design, **36**, 874 (2012).
[2] S. Pournaderi, S. Mahdavi, F. Akhlaghi, Powder Technology, **229**, 276 (2012)
[3] Majid Hoseinia, Mahmood Meratian, Journal of Alloys and Compounds **471**, 378 (2009).
[4] A.M. Al-Qutub, I.M. Allam, T.W. Qureshi, Journal of Materials Processing Technology, **172**, 327 (2006).
[5] X.P. Zhang, L. Ye, Y.W. Mai, G.F. Quan, W. Wei, Composites: Part A **30**, 1415 (1999)
[6] A.R.I. Khedera, G.S. Marahleh, D.M.K. Al-Jamea, Jordan Journal of Mechanical and Industrial Engineering, **5,** 533 (2011).
[7] L.E.G. Cambronero, E. Sanchez, J.M. Ruiz-Roman, J.M. Ruiz-Prieto, Journal of Materials Processing Technology **143-144**, 378 (2003).
[8] Rupa Dasgupta, Humaira Meenai, Materials Characterization **54**, 438 (2005).
[9] A.D.P. LaDelpha, H. Neubing, D.P. Bishopa, Materials Science and Engineering, A **520**, 105 (2009).
[10] J. Corrochano, M. Lieblich, J. Ibáñez, Composites Science and Technology, **69**, 1818 (2009).
[11] B. Torres, M. Lieblich, J. Ibanez, A. Garcia Escorial, Scripta Materialia **47**, 45 (2002).
[12] L. Mateusz, K. Jan, Acta Polytechnica, 2012, Vol. 52.
[13] Ch. Normah, M. N. Derman, N. M. Shima, M. Z. Kasmuin, S. B. Jamaludin, National Metallurgical Conference 2007 (NMC 2007) 26-27 November, Puteri Pasific Hotel, Johor Malaysia
[14] N.P. Cheng, S.M. Zeng, Z. Y. Liu, Journal Of Materials Processing Technology **202**, 27 (2008).
[15] Mehdi Rahimian, Naser Ehsani, Nader Parvin, Hamid reza B., Journal of Materials Processing technology **209**, 5387 (2009).
[16] Haider T. Naeem, Kahtan S. Mohammad, Digest Journal of Nonmaterial and Bio structures **8**, 1621 (2013)
[17] Haider T. Naeem, Kahtan S. Mohammed, Materials Sciences and Applications **4**, 704 (2013).
[18] Li Guo, Zhang Xin, Li Peng, You Jiang, Trans. Nonferrous Meta. Soc. China **20**, 935 (2010).
[19] N. Parvin, M. Rahimian, Acta Physica Polonica A, 2012, 121, Proceedings of the International Congress on Advances in Applied Physics and Materials Science, Antalya 2011.
[20] Mohsen Hossein-Zadeh, Omid Mirzaee, Peyman Saidi, Materials and Design **54**, 245 (2014).
[21] Z. Zhang, D.L. Chen, Scripta Materialia **54**, 1321 (2006).